Available online at www.sciencedirect.com
ScienceDirect
Journal of the European Ceramic Society 31 (2011) 977–981
www.elsevier.com/locate/jeurceramsoc

Short Communication

The effect of alumina contamination from the ball-milling of fused silica on the high temperature properties of injection moulded silica ceramic components

P.J. Wilson [a,b,*], S. Blackburn [a], R.W. Greenwood [a], B. Prajapti [b], K. Smalley [b]

[a] *University of Birmingham, School of Chemical Engineering, Edgbaston, Birmingham B15 2TT, United Kingdom*
[b] *Ross Ceramic Ltd., Derby Road, Denby DE5 8NX, United Kingdom*

Received 3 September 2010; received in revised form 3 December 2010; accepted 14 December 2010
Available online 15 January 2011

Abstract

The amount of alumina contamination present in ball-milled silica powders has been shown to increase with increased mill time for materials manufactured during the same time period. This alumina contamination level has also been observed to vary depending on the date, and possibly the state of repair, of the ball mill itself. The associated alumina level has been shown to significantly influence the high temperature properties (at 1475 °C) of the materials, with high contamination levels not only resulting in increased flexural strength and creep resistance, but also increasing the thermal contraction of the materials when dilatometer measurements were performed to 1600 °C.

Keywords: Al_2O_3; SiO_2; Mechanical properties; Impurities; Milling

1. Introduction

It is well known that, during grinding operations, such as the manufacturing technique of ball milling, contamination from wear of the milling media and lining of the mill itself can generate contamination which is subsequently included into the mill products.[1,2] The exact amount of contamination depends on the length of time a material is milled, the size of the mill media, the mill media material, the mill lining material, the material being milled and the current wear of the media itself. This last point is due to full scale industrial mills adding media to maintain an equilibrium mass of media inside the mill, resulting in uneven, and non-reproducible, wear of the mill media present at any given time.[3] Wear during dry grinding has been shown to be entirely due to abrasion and erosion of the mill media and mill lining.[4]

The contamination from this operation can be of significance, especially in materials that rely on their purity for successful operation. The contamination from ball milling has been shown to affect high temperature properties in some ceramic materials,[5] but not for silica based ceramics used in the investment casting environment.

Alumina is a common additive to silica-based ceramics and glasses. Alumina and silica in stoichiometric ratios and at high temperatures form mullite, $Al_{4+2x}Si_{2-2x}O_{10-x}$, with x ranging between 0.2 and 0.9, depending on the formation temperature and atmosphere.[6] It has been reported that alumina can prevent the devitrification of silica. However, this is in common glasses and is due to a strong coupling reaction between Al^{3+} and Na^{+}.[7,8] Alumina prevents the transport of alkaline ions through the silica structure that are necessary for cristobalite formation. However, alumina does not directly affect the crystallisation temperature of cristobalite, which is maintained at approximately 1200 °C,[9] but alumina can increase the crystallisation rate in small concentrations.[10]

Cristobalite has been reported to form a glassy phase with α-alumina at ≈1500 °C that expedites the formation of mullite and aids densification at elevated temperatures. However, the phase diagram of the ideal SiO_2–Al_2O_3 system shows that a

* Corresponding author at: University of Birmingham, School of Chemical Engineering, Edgbaston, Birmingham B15 2TT, United Kingdom. Tel.: +44 01214711922.
E-mail addresses: pjw256@gmail.com, pwilson@rossceramics.co.uk (P.J. Wilson).

0955-2219/$ – see front matter © 2011 Elsevier Ltd. All rights reserved.
doi:10.1016/j.jeurceramsoc.2010.12.016

Table 1
List of the properties of the silica powders that were used in this trial.

Crystallinity (%)	0
TiO_2%	0.02
Al_2O_3%	0.09–0.16
Fe_2O_3%	0.02
Na_2O%	0.01
Total contamination (%)	0.14–0.21
Surface area (m^2/g)[a]	0.67
D_{50} (μm)[b]	24.0

[a] Measured using a Micromeritics ASAP 2010 gas adsorption machine.
[b] Measured using a Malvern Mastersizer 2000 laser diffraction particle size analyser.

liquid phase should not form below 1587 ± 10 °C.[11] Contamination within real systems would depress this temperature leading to the formation of liquid phases below that of the idealised Al_2O_3–SiO_2 system.

In silica systems Al_2O_3 is a known network former. The presence of Al_2O_3 in a silica melt increases the viscosity according to an Arrhenian relationship[12] up to the liquidus temperature. Hence, the presence of alumina, even in small quantities is likely to have an effect on ceramic properties, particularly at elevated temperatures.

2. Materials and methods

2.1. Ceramic materials

Four ceramic materials were obtained from Ross Ceramics Ltd., all of which used only silica in their formulation. The materials were created using a number of powders supplied at different dates that had different levels of alumina present. The materials were obtained from Unimin Corporation, Camden, Tennessee, in a variety of particle size distributions that were obtained by ball milling with alumina grinding media and in an alumina lined mill. The use of alumina grinding media caused this level of alumina contamination to vary. However, the level of contamination from other minerals was constant, see Table 1.

The supplied powders were mixed to create a specific particle size distribution (PSD), within ±5% for the D_{90} and D_{10} and ±10% for the D_{50}, to avoid significant PSD effects. The properties of these mixed powders are shown in Table 1. The final alumina amounts present in each material were then a consequence of meeting this PSD with silica powders that had different starting alumina contamination levels and were not designed specifically to have set concentrations of alumina. The amount of alumina detected in each material, by XRF, is shown in Table 2.

The materials were supplied as fired test bars with dimensions, 100 mm × 12 mm × 4 mm. The test bars were fired up to 1200 ± 25 °C and two fires were performed on each material, in order that variation from the firing of the materials was included in the data.

Table 2
Alumina contamination (%) of the 4 silica ceramic materials.

Material	Al_2O_3 contamination (%)
1	0.088
2	0.132
3	0.152
4	0.162

2.2. X-ray fluorescence (XRF)

The XRF characterisation was conducted by Ceram, UK, and was performed by forming the sample into a fused cast bead using Spectroflux 100B (1 part $Li_2B_4O_7$ to 4 parts $LiBO_2$ by weight) at a ratio of 5:1 to the sample, this allowed volatile components like Na_2O, K_2O, SO_3 and F to be retained. The sample preparation and analysis was conducted in accordance with the BS ISO 12677 standard for XRF analysis.

2.3. Mechanical tests

Three point bend tests were performed at 1475 °C using three point bend fixtures comprising re-crystallised alumina push rods and a custom furnace. This system was capable of isothermal hold temperatures up to 1500 °C. The span of the two support rods was 80 mm with a rounded knife edge and the test was performed at 1 mm min^{-1}.

Creep tests at 1475 °C were performed on the same rig as that used for the high temperature flexural tests. The load rate applied was 1 mm min^{-1} until a load of 3.2 N was achieved. This load was then held for 5 min and the total deflection of the test piece was recorded.

2.4. Dilatometry

Dilatometer measurements were conducted in a vertical dilatometer. Specimens were ground to approximately 20 mm × 4 mm × 4 mm.

Measurements were performed to 1600 °C to reveal the presence of any phase changes that may occur during casting and specifically to determine if the phase eutectic at 1587 °C of the SiO_2–Al_2O_3 systems was affecting material properties. Specimens were ramped to this temperature at 6 °C min^{-1} and held for 15 min before being cooled at 14 °C min^{-1}, this was as fast as the furnace would allow.

The Total Thermal Contraction (TTC) during the test was taken by measuring the relative length change at 1250 °C during the heat-up of the material and again at 1250 °C during the cooling down of the sample after the dwell at 1600 °C.

2.5. SEM analysis

Scanning election microscopy was performed on a JEOL 6060 SEM. Powders were coated with gold and a 20 kV beam was used with a spot size of 59.

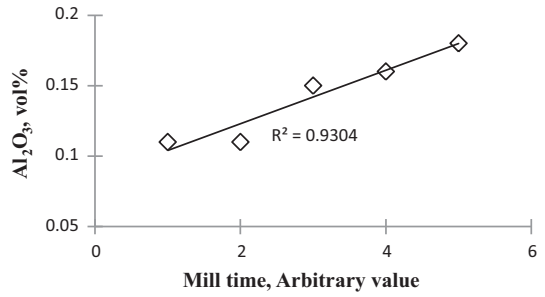

Fig. 1. Alumina content of the silica powders as a function of mill time.

3. Results and discussion

3.1. Al_2O_3 content of silica powders

Several grades of fused silica were analysed for their alumina content. The finer the material, the longer the mill time attributed to the material. Hence, an arbitrary value of time was associated with each fused silica grade, with 1 being the coarsest material, milled for the least time, and 5 being the finest material, milled for the longest. The level of alumina can be seen to increase linearly for increasing mill time indicating increased abrasion from the mill media and lining, see Fig. 1.

The finest and the second from coarsest grade of silica powder were then air classified into various size ranges that were as monomodal as possible. These powders were then re-analysed for their alumina contamination. The amount of alumina present can be seen to increase considerably with decreasing particle size, see Fig. 2. The level of TiO_2 and Fe_2O_3, two common contaminants in the silica source material, can be seen to remain unchanged, despite the air-classification machinery being made from steel. This indicates that the alumina is separate from the source silica and introduced predominantly as fine attrition derived products.

Since the alumina is derived from an attrition process it was likely adhered to the surface of the larger silica particles present, because the small sizes would tend to flocculate, evidence of which was possibly seen under SEM inspection but was unconfirmed with EDX analysis, see Fig. 3. It was also possible that there was a fine portion of free, abraded, alumina in the fine

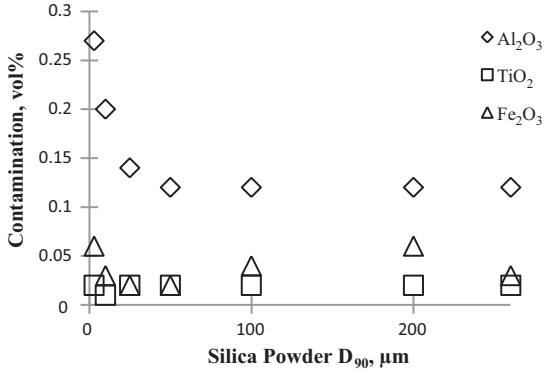

Fig. 2. Variation of three common contaminants in fused silica, Al_2O_3, TiO_2 and Fe_2O_3, determined by XRF, of the air classified silica powders vs. the D_{90} of the associated powder.

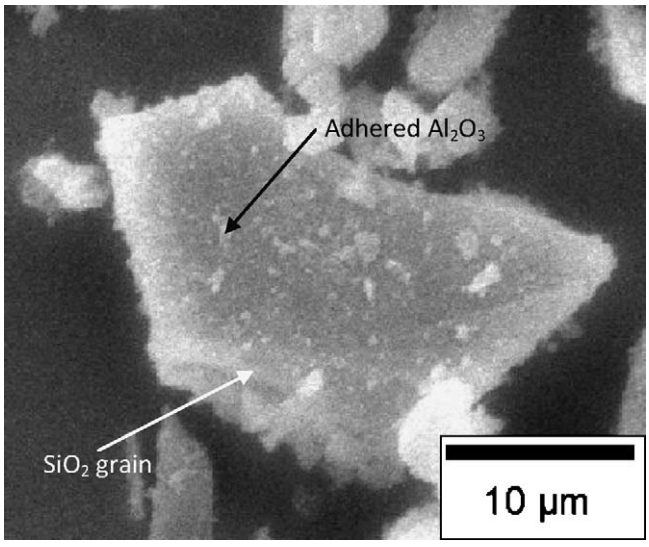

Fig. 3. SEM micrograph of the 25 µm air-classified silica powder showing small particles adhered to the surface, possibly alumina contamination.

silica component that was air-classified along with this to give the higher amounts in the low particle size range. However, the higher surface area of the finer silica likely had more alumina adhered to the surface, resulting in high amounts being present in the finer particle sizes.

A significant increase in surface area was observed for the finer air-classified silica, see Fig. 4. Hence, it was likely that the increase in alumina observed in the finer air classified silica was a function of the surface area of the silica powder itself and not a fine, free, alumina component within the powder. However, the alumina contamination, $C_{Al_2O_3}$, is not directly proportional to the increased surface area, S, according to[4] Eq. (1).

$$C_{Al_2O_3} = C_{sp}S \quad (1)$$

The specific contamination, C_{sp}, is larger for the powders with less surface area and smaller for the finest powder, see Fig. 5. This suggests that with this material a higher surface area does not necessarily imply a vastly increased contamination. This may be due to the cushioning effect of fine silica powder on the outside of the mill media preventing erosion and abrasion, and thus reducing the specific contamination for materials with higher surface area.

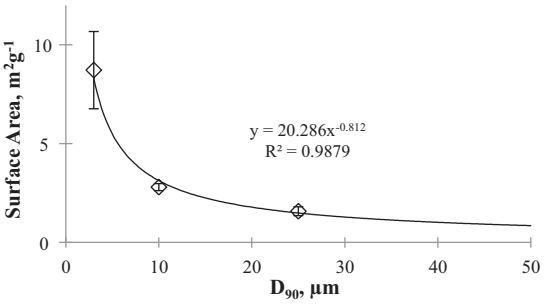

Fig. 4. Surface area of the 3 finest air-classified silica distributions.

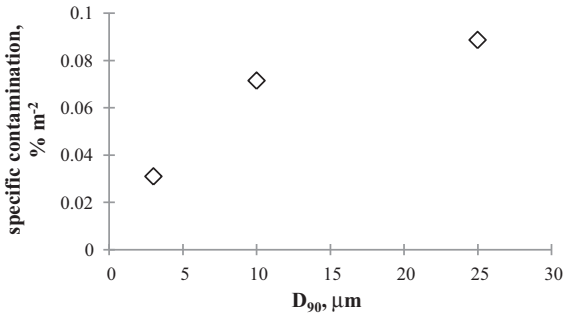

Fig. 5. Specific surface contamination for the 3 finest air classified silica powders.

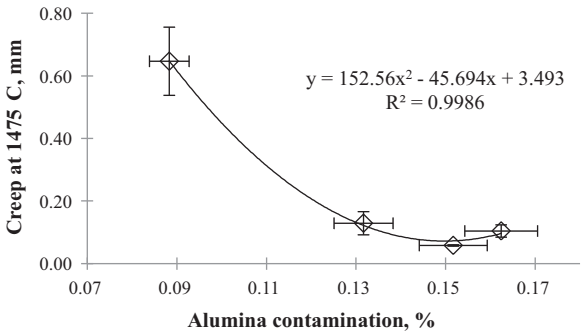

Fig. 7. Creep of the silica materials with different alumina contamination levels.

3.2. The effect of Al_2O_3 contamination on flexural strength at 1475 °C

There appears to be a quadratic relation of increasing hot strength with increasing alumina contamination up to a certain level, of approximately 0.14% and then either a plateau in flexural strength or a reduction, Fig. 6. Small amounts of alumina contamination yield a significantly weaker material; this was probably due to the alumina present acting as a network former, strengthening the grain boundaries of the material.

Beyond a certain level of alumina addition through milling there would be less of an effect since the surface of the silica grains would be sufficiently coated with the alumina and any further additions would either have little additional effect or be a hindrance, by introducing too much of an alumina–silica mixture at the grain boundaries.

3.3. The effect of Al_2O_3 contamination on creep properties at 1475 °C

The creep resistance of these materials increases with increased alumina contamination indicating that the alumina has indeed acted as a network former. The lowest creep value was observed with approximately 0.15% Al_2O_3, a similar level to that of the maximum flexural strength seen in the previous section, see Fig. 7.

The material with a low alumina contamination level was much more susceptible to grain boundary creep deformation than those with high alumina contamination. The slight inflection in the data fit could be an artefact since the creep resistance may plateau beyond 0.15%. However, a large amount of alumina could result in increased apparent ductility at 1475 °C by introducing a significant SiO_2–Al_2O_3 mixture at the grain boundaries.

3.4. The effect of Al_2O_3 contamination on Total Thermal Contraction to 1600 °C

The Total Thermal Contraction (TTC) during the dilatometry measurement to 1600 °C would be expected to show a considerable contraction with larger amounts of alumina due to the phase eutectic at 1587 ± 10 °C. Fig. 8 shows that this was observed for the material with an intermediate level of alumina contamination, approximately 0.13%. This then reduced with further addition. The material with the least alumina contamination, predictably, contracted the least.

The liquid phase formed at 1587 °C with the presence of alumina would cause contraction at temperatures approaching and exceed this. It was possible that, with alumina amounts exceeding approximately 0.13%, mullite was being formed at the grain boundaries that limited the effect of the liquid phase, since mullite would be expected to form above 1500 °C in this system. Below 0.13% the formation of mullite crystals was probably too small to have an effect on grain boundary properties.

The formation of mullite may not have been favourable or at a sufficiently fast rate as to have an effect on the properties at 1475 °C, which would explain the only subtle inflection of the flexural strength and creep properties were seen beyond a critical level.

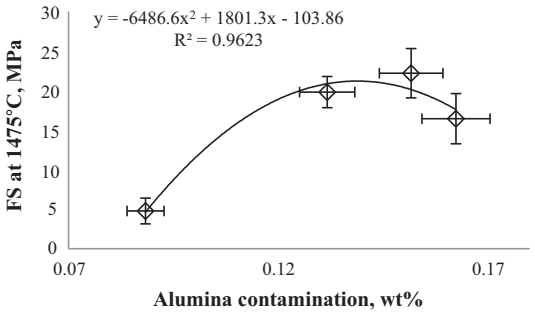

Fig. 6. Flexural strength (FS) at 1475 °C for the 4 material created with different levels of alumina contamination.

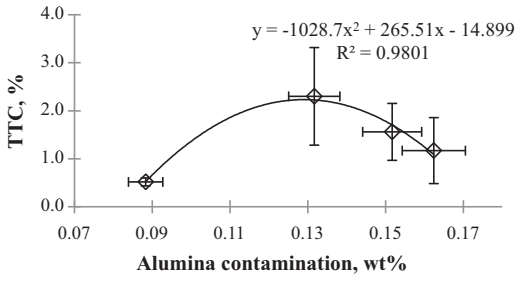

Fig. 8. Total Thermal Contraction (TTC) during dilatometer test to 1600 °C for the silica materials with different alumina contamination levels.

4. Conclusion

Alumina contamination has been shown to have a significant effect at both 1475 °C for mechanical tests and 1600 °C for dilatometry measurements.

The silica ceramic tested was shown to increase in both strength and creep resistance at 1475 °C with increasing alumina contamination up to a level of 0.145%. This has implications for materials that depend on their ability to remain structurally stable at high temperature since they must contain a consistent level of Al_2O_3 contamination in order for their properties to remain stable. The alumina was probably acting as a network former with the silica, acting to strengthen the inter-granular bonds.

Dilatometry measurements indicated that greater amounts of alumina increased the total contraction that would be expected for a material up to a critical amount of approximately 0.13%, indicating increased liquid phase sintering. Beyond the critical amount of alumina the contraction began to decrease, indicating a reduction in liquid phase sintering, possibly caused by an increase in mullite formation between the grain boundaries.

Acknowledgements

This research was made possible through funding from the EPSRC and Ross Ceramics Ltd., UK, and support from the University of Birmingham Centre for Formulation Engineering.

References

1. Suzuki Y, Azuma K, Kuwahara N. Increase of impurity during fine grinding. *Adv Powder Technol* 1990;**1**:51–60.
2. Gammage RB, Glasson DR. Wear of mill components during the ball milling of calcium carbonate. *J Colloid Interface Sci* 1979;**71**:522–5.
3. Austin LG, Klimpel RR. Ball wear and ball size distributions in tumbling ball mills. *Powder Technol* 1985;**41**:279–86.
4. Tkacova K, Stevulova N, Lipka J, Sepelak V. Contamination of quartz by iron in energy-intensive grinding in air and liquids of various polarity. *Powder Technol* 1995;**83**:163–71.
5. Perez-Rodriguez JL, Perez-Maqueda LA, Justo A, Sanchez-Soto PJ. Influence of grinding contamination on high-temperature phases of pyrophyllite. *J Eur Ceram Soc* 1993;**11**:335–9.
6. Schneider H, Schreuer J, Hildmann B. Structure and properties of mullite—a review. *J Eur Ceram Soc* 2008;**28**:329–44.
7. Chao CH, Lu HY. Beta-cristobalite stabilization in ($Na_2O + Al_2O_3$)—added silica. *Metall Mater Trans A* 2002;**33A**:p2703.
8. Jean J, Chang CR, Chang RL, Kuan TH. Effect of alumina particle size on the prevention of crystal growth in low-K silica dielectric composites. *Mater Chem Phys* 1994;**40**:50–5.
9. Tezuka N, Low IM, Davies IJ, Prior M, Studer A. In situ neutron diffraction investigation on the phase transformation sequence of kaolinite and halloysite to mullite. *Physica B* 2006;**385–386**:555–7.
10. Brown SD, Kistler SS. Devitrification of high SiO_2 glasses of the system Al_2O_3–SiO_2. *J Am Ceram Soc* 1959;**42**:263–70.
11. Nurishi Y, Pask JA. Sintering of alpha-Al_2O_3—amorphous silica compacts. *Ceram Int* 1982;**8**:57–9.
12. Mysen BO, Virgo D. Viscosity and structure of iron and aluminium-bearing calcium silicate melts at 1 atm. *Am Miner* 1985;**70**:487–98.